

## Research Article

# Nonlinear Analysis of Flexible Pile near Undrained Clay Slope under Lateral Loading

Chong Jiang , Yu Li, Lin Liu , and Hang Lin 

School of Resources and Safety Engineering, Central South University, Changsha 410083, Hunan, China

Correspondence should be addressed to Lin Liu; [liulin9358@csu.edu.cn](mailto:liulin9358@csu.edu.cn) and Hang Lin; [linhangabc@126.com](mailto:linhangabc@126.com)

Received 3 September 2018; Accepted 25 October 2018; Published 21 November 2018

Guest Editor: Xihong Zhang

Copyright © 2018 Chong Jiang et al. This is an open access article distributed under the Creative Commons Attribution License, which permits unrestricted use, distribution, and reproduction in any medium, provided the original work is properly cited.

In this paper, a method is developed for nonlinear analysis of laterally loaded long-flexible pile near undrained clay slope. The ideal elastic-plastic  $p$ - $y$  curve model is used as the basic calculation model to study the pile-soil interaction system. To consider the slope effect on the soil resistance along with pile length, related reduction function expressions of soil resistance are selected by assessing the existing methods. A finite difference iteration scheme is proposed to solve the pile's deflection curve equations to obtain nonlinear response of pile. The developed method is validated by comparing its results with the existing method, which shows a good agreement. A number of parameters analyses are carried out, and effects of different influence factors on laterally loaded pile are further discussed.

## 1. Introduction

Pile foundations are widely used to support structures such as bridges, high-rise buildings, transmission line towers, and traffic signs that are frequently constructed near or in a natural or man-made slope [1]. The pile foundations are often subjected to static lateral loading in many cases. For the design needs of pile foundations, many scholars have conducted a lot of research on laterally loaded piles in horizontal ground. The most commonly used theoretical method for laterally loaded pile in the current design approach is the well-known subgrade reaction method, which considers the pile as a beam supported by a series of nonlinear soil springs. The lateral load transfer curves (i.e.,  $p$ - $y$  curves) are often used to describe the load-deformation characteristics of nonlinear soil springs. Different criteria for developing  $p$ - $y$  curves under many cases, including soil types, soil strength, loading conditions, pore water pressure conditions in soil, etc., have been proposed by several investigators (Matlock [2], Reese et al. [3, 4], Reese and Welch [5], Gabr et al. [6], Fan and Long [7], and some others) mainly through the back analyses of lateral load tests, and these typical  $p$ - $y$  curves have been incorporated into the API specification as a reference for

the design of pile foundation structure in offshore engineering [8]. Subsequently, Wang et al. [9, 10] proposed a new  $p$ - $y$  curve method of laterally loaded pile in clay based on the analyses and calculation of the existing field test data through the stress-strain relationship. Wang and Yang [11] used the construction parameters to normalize the different forms of  $p$ - $y$  curves in sand and then proposed a hyperbolic model. An ideal elastic-plastic  $p$ - $y$  calculation model for clay was also proposed based on a comprehensive analysis of the measured  $p$ - $y$  curves in clay [12]. Zhou et al. [13] proposed a new empirical formula for the  $p$ - $y$  curves of ultralong PHC pipe piles in soft clay based on the analyses of the relationship between ultimate soil resistance and some geotechnical parameters from lateral pile load test.

For laterally loaded pile near slopes, the stress environment of the pile foundation becomes, due to the lack of soil volume in front of the pile, more complex, and the lateral load-bearing characteristics and failure model are different from that pile in horizontal ground [14–16]. Thus, the existing theoretical calculation methods for laterally loaded pile in horizontal ground are not suitable for pile near slopes. Available studies about the lateral loading capacity behavior of piles in sloped ground mainly focus on model tests and numerical simulation (Georgiadis [17, 18]; Muthukkumaran

et al. [19]; Zhang et al. [20]; Yin et al. [21]; Gao et al. [22]), but rare in the theoretical calculations.

This paper attempts to present a method for the nonlinear analysis of laterally loaded long-flexible piles near sloped ground. For the developed method, the ideal elastic-plastic  $p$ - $y$  curve model is used as the basic calculation model to study the pile-soil interaction system. To consider the slope effect on the soil resistance along with pile length, related reduction function expressions of soil resistance are selected by assessing the existing methods. A finite difference iteration scheme is then proposed to solve the pile's deflection curve equations to obtain nonlinear response of pile. To validate the developed method, it is first compared to pile test and three-dimensional numerical finite element analysis results, and the results show that the developed method can provide satisfactory prediction of the response of laterally loaded pile near clay slopes. Then, it is applied to analyze the parametric influence law, and the nonlinear response results of pile near clay slope under different influence factors are obtained.

## 2. Method of Analysis

**2.1. Mechanical Analysis Model.** Currently,  $p$ - $y$  curve methods were used by many researchers to study the nonlinear response characteristics of the laterally loaded pile in horizontal ground. Zhu [23] conducted extensive analysis of laterally loaded pile in horizontal ground by using the elastic-plastic  $p$ - $y$  curve model and suggested that choosing reasonable model parameters can obtain realistic results. In succession, the general calculation form of the ideal elastic-plastic  $p$ - $y$  curve method in clay (Figure 1), based on this, was given by Wang and Yang [12] as follows:

$$p = \begin{cases} Ky, & y \leq y_u, \\ p_u, & y > y_u, \end{cases} \quad (1)$$

where  $K$  = initial slope of the  $p$ - $y$  curve,  $y$  = lateral displacement of pile,  $p_u$  = ultimate soil resistance (per unit pile length), and  $y_u$  = allowable lateral displacement for soil in elastic state.

In order to consider the influence of slope effects, the analysis model for laterally loaded pile near sloped ground is set up as shown in Figure 2.

Where  $L$  = buried pile length,  $H_0$  = lateral load acting on the pile top,  $B$  = distance from the pile shaft to the slope crest,  $\theta$  = slope angle,  $D$  = pile diameter, and  $e$  = height of the load above the clay surface.

**2.2. Assumptions.** To facilitate the establishment of method, assumptions and statements are made in advance.

- (1) The cross-sectional shape of pile at all depths is equal; besides, both the pile and the soil are homogeneous and isotropic materials
- (2) The ultimate lateral soil resistance ( $p_u$ ) varies nonlinearly with depth
- (3) Considering the slope effect, the initial stiffness ( $K$ ) and the ultimate lateral soil resistance ( $p_u$ ) should be reduced within a certain depth

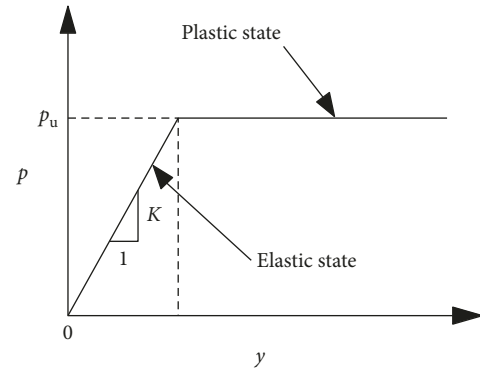


FIGURE 1: Ideal elastic-plastic  $p$ - $y$  curve.

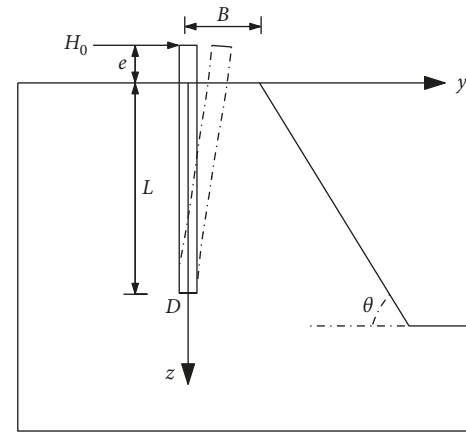


FIGURE 2: Analysis model definition.

- (4) Assume that clay slope is stable, and the slope destruction and instability are not taken into consideration during the process of calculation

**2.3.  $p$ - $y$  Curve Model of Laterally Loaded Pile near Slope.** With the basic assumptions in Section 2.2, equation (1) is then modified to obtain the new ideal elastic-plastic  $p$ - $y$  curves as follows:

$$p = \begin{cases} \mu(z)Ky, & y \leq y_u, \\ p_{su}(\theta, B, z), & y > y_u, \end{cases} \quad (2)$$

where  $\mu(z)$  is the reduction function of the soil lateral initial stiffness ( $K$ );  $p_{su}(\theta, B, z)$  is the ultimate lateral soil resistance per unit pile length under the condition of pile near slope.

Allowable lateral displacement of  $y_u$  can be obtained according to equation (2):

$$y_u = \frac{p_{su}(\theta, B, z)}{\mu(z)K}. \quad (3)$$

## 3. Initial Stiffness $K$

The problem of choosing the initial stiffness of the soil in the  $p$ - $y$  curve has always been focused on by investigators. Many scholars believed that the lateral initial stiffness  $K$  of clay remains constant in all depth. This paper adopts the initial

stiffness recommended by Rajeshree and Sitharam [24] as follows:

$$K_i = \frac{1.3E_i}{1-\nu_s^2} \left( \frac{E_i D^4}{E_p I_p} \right)^{1/12}, \quad (4)$$

where  $\nu_s$ ,  $E_p I_p$  is Poisson's ratio of soil and pile bending rigidity, respectively.

According to the Kondner [25], the initial elasticity modulus can be related to elasticity modulus  $E_{50}$  under the 50% failure stress, and the elasticity modulus at deviatoric stress can be expressed by

$$E_s = E_i \left( 1 - \frac{R_f \sigma}{\sigma_f} \right), \quad (5)$$

where  $\sigma$  is deviation stress,  $\sigma_f$  is deviatoric failure stress,  $R_f$  is the ratio of the deviatoric failure stress over the ultimate deviatoric stress, generally taken as 0.8,  $E_i$  is the initial elastic modulus, and  $\sigma/\sigma_f = 0.5$ .

For undrained loading, we have  $\nu_s = 0.5$ . The elastic modulus of the clay is represented by the deformation modulus  $E_{50}$  under the 50% failure stress of the reaction soil, and  $E_i = 1.67 E_{50}$  is satisfied. The above expression can be used to derive the initial stiffness ( $K$ ) of clay under undrained conditions:

$$K = 3E_{50} \left( \frac{E_{50} D^4}{E_p I_p} \right)^{1/12}. \quad (6)$$

#### 4. Reduction Function of Initial Stiffness $u(z)$

For near-slope laterally loaded pile, the initial stiffness of the soil is also affected by the slope [17, 18, 22]. Georgiadis and Georgiadis [18] gave the reduction function for the initial stiffness of clay within the shallow foundation under undrained loading condition:

$$u(z) = \cos \theta + \frac{1 - \cos \theta}{6} \left[ \frac{z}{D} + \left( \frac{B}{D} - 0.5 \right) \tan \theta \right] \leq 1. \quad (7)$$

#### 5. Ultimate Soil Resistance of Clay $p_{su}$

Several methods are available for determining the ultimate soil lateral resistance  $p_u$  to piles in cohesive soil [2, 4–6, 10, 12]. It is generally believed that the ultimate resistance ( $p_u$ ) of clay depends mainly on the type of failure mechanism at a certain depth of the soil. The normative formula in API design code for horizontal ground is given in equation (8):

$$N_p = 3 + \frac{\gamma' z}{c_u} + J \frac{z}{D} \leq 9, \quad (8)$$

$$p_u = N_p c_u D, \quad (9)$$

where  $N_p$  is ultimate capacity coefficient of clay,  $c_u$  is undrained shear strength of clay,  $\gamma'$  is effective bulk density of clay, and  $J$  is dimensionless experience coefficient, its value ranges from 0.25 to 0.5.

To consider slope effect on the ultimate soil resistance, the following expression proposed by [18] is used to calculate the ultimate soil resistance  $N_{sp}$ :

$$N_{sp} = \begin{cases} N_{pu} - (N_{pu} - N_{p0}) e^{-\lambda(z/D)}, & z \leq z_c, \\ N_{pu} - (N_{pu} - N_{pc}) e^{-\lambda \alpha_\theta (z-z_c)/D}, & z > z_c, \end{cases} \quad (10)$$

$$\alpha_\theta = 1 - \frac{\sin \theta (1 + \sin \theta)}{2}, \quad (11)$$

$$z_c = \left[ 8.5 - 10 \log_{10}^{(8-b/D)} \right] D, \quad (12)$$

$$N_{pu} = \pi + 2\Delta + 2 \cos \Delta + 4 \left( \cos \frac{\Delta}{2} + \sin \frac{\Delta}{2} \right), \quad (13)$$

where  $z_c$  is the certain critical depth,  $\alpha_\theta$  is the parameter related to the slope,  $N_{pu}$  is the ultimate lateral bearing capacity factor. Besides,  $\Delta = \sin^{-1} \alpha$  and  $\lambda = 0.55 - 0.15\alpha$ , both are dimensionless coefficients;  $N_{p0}$  is the lateral bearing capacity factor at ground surface,  $N_{p0} = 2 + 1.5 \alpha$ .  $\alpha$  is the adhesion coefficient, and its value ranges from 0~1;  $N_{pc}$  is the ultimate soil resistance at a certain critical depth.

According to equations (9)–(13), the ultimate soil resistance of clay  $p_{su}$  for undrained conditions can be expressed as

$$P_{su} = N_{sp} C_u D. \quad (14)$$

### 6. FDM Solution of the Proposed Method

**6.1. Establishment of Calculation Model.** A simplified calculation model can be established as shown in Figure 3.

Select a microunit of the pile for force balance analysis. It is stated here that the bending moment is positive in the counterclockwise rotation direction, and the normal of the shear force is positive in the positive direction of the  $z$  axis. The shear force is positive in the negative direction of the  $y$  axis. Then the equation for the deflection of the pile can be derived as follows:

$$E_p I_p \frac{d^4 y}{dz^4} + p(y, z) = 0, \quad (15)$$

where  $E_p I_p$  is the pile bending stiffness,  $p(y, z)$  is the soil resistance distributed along pile length, which can be obtained from the previous  $p$ - $y$  curve, and the positive direction is positive direction of the  $y$  axis.

Boundary restrictions must be determined to solve the above-mentioned deflection differential equation. In this paper, the boundary conditions of the pile are determined: the pile top is free and the pile bottom is fixed, and the corresponding deflection differential equations are as follows:

Free pile head:

$$\begin{cases} E_p I_p y'' \Big|_{z=0} = M_0, \\ E_p I_p y''' \Big|_{z=0} = H_0. \end{cases} \quad (16)$$

Fixed pile bottom:

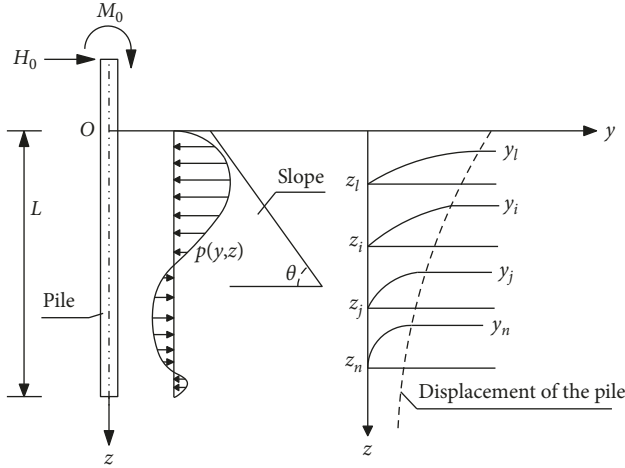


FIGURE 3: Simplified calculation model of near-slope pile.

$$\begin{cases} E_p I_p y'' \Big|_{z=L} = 0, \\ E_p I_p y''' \Big|_{z=L} = 0. \end{cases} \quad (17)$$

**6.2. Differential Format Derivation and Solution.** The finite difference method principle is used to discrete the buried section  $L$  into  $n$  segments, each of which is  $s = L/n$ . The top node is denoted as 0, and the bottom of the pile is marked as  $n$ . In order to improve the simplicity of the finite difference operation, four virtual nodes,  $-2, -1, n+1, n+2$  are added at the top of pile and the bottom of the pile, respectively. The displacement of the  $i$ th node is  $y_i$  is shown in Figure 4.

For a pile, there exists  $(n+5)$  differential equations after the discrete division, and four extra known differential equations can be derived in combination with the boundary conditions, thereby establishing the pile displacement node vector  $\{y_i\}$  and further solving the pile displacement.

Substituting the fourth derivative of pile microelement in equation (15), the differential equation for each element of the pile can be derived:

$$y_{i+2} - 4y_{i+1} + 6y_i - 4y_{i-1} + y_{i-2} + \frac{s^4}{E_p I_p} p(y_i, z) = 0. \quad (18)$$

In combination with equation (2), equation (18) can be transformed into the following two forms according to the allowable displacement  $y_u$ :

(1)  $y \leq y_u$

$$\begin{cases} y_{i+2} - 4y_{i+1} + (6 + mu(z)K)y_i - 4y_{i-1} + y_{i-2} = 0, \\ m = \frac{s^4}{E_p I_p}. \end{cases} \quad (19)$$

(2)  $y > y_u$

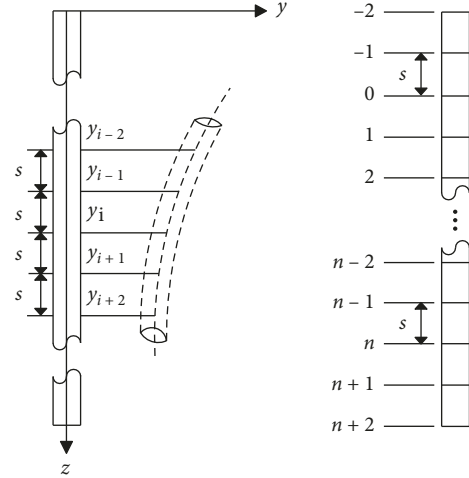


FIGURE 4: Finite difference method cell division.

$$\begin{cases} y_{i+2} - 4y_{i+1} + 6y_i - 4y_{i-1} + y_{i-2} + mN_{sp}C_uD = 0, \\ m = \frac{s^4}{E_p I_p}. \end{cases} \quad (20)$$

Similarly, in terms of equations (16) and (17), the differential form of the boundary conditions can be derived:

$$\begin{cases} y_2 - 2y_1 + 2y_{-1} - y_{-2} = 2H_0 \frac{s^3}{E_p I_p}, \\ y_1 - 2y_0 + y_{-1} = M_0 \frac{s^2}{E_p I_p}, \\ y_{n+1} - 2y_n + y_{n-1} = 0, \\ y_{n+2} - 2y_{n+1} + 2y_{n-1} - y_{n-2} = 0. \end{cases} \quad (21)$$

According to the differential equations from equation (21) of the boundary conditions,  $(n+1)$  unknown differential equations are combined to obtain the displacement of the pile matrix, the corresponding pile displacement solution equations can be expressed as

$$[K_n]\{y\} = \{F\}, \quad (22)$$

where  $[K_n]$  is the stiffness matrix of pile, which is divided into two type stiffness matrix of  $[K_1]$  and  $[K_2]$  according to the elastic state and plastic state of the soil along the pile length, respectively;  $\{y\}$  is the pile displacement node vector;  $\{F\}$  is external load vector, which is controlled by boundary conditions and is also divided into two type vector of  $\{F_1\}$  and  $\{F_2\}$  correspond to  $[K_1]$  and  $[K_2]$ , respectively.

In most practical projects, the maximum bending moment section is regarded as the most dangerous cross section

of the pile design. Here, the differential form of the solution of the bending moment is listed as

$$M_i = \frac{(y_{i-1} - 2y_i + y_{i+1})E_p I_p}{s^2} \quad (23)$$

According to the basic solution ideas of equation (22), a MATLAB iterative code is developed to solve the response behavior of pile, and the flow chart of iterative calculation is shown in Figure 5.

## 7. Validation to Previous Studies

The feasibility of the proposed method is validated in this section to some previous studies, which are well documented in the literature. This method is introduced as input into MATLAB to calculate the response of each pile. The geometrical characteristics (pile length  $L$ , pile diameter  $D$ , distance from the pile shaft to the slope crest  $B$ , bending stiffness of the pile  $E_p I_p$ , and slope angle  $\theta$ ) and the soil properties (undrained shear strength  $c_u$ , secant modulus  $E_{50}$ , effective bulk density  $\gamma$  or  $\gamma'$ , and cohesion coefficient  $\alpha$ .) are summarized in Table 1 for each previous study considered.

*Case 1.* The computed pile responses are compared to the pile test results and to the pile responses computed with the same computer code using as input the Matlock [2], Reese and Welch [5], Bhushan et al. [26], Stevens and Audibert [27]. The Shanghai pile tests, as shown in Figure 6, reported by the literature [28], involved lateral loading of piles in level ground. It can be seen that despite the small discrepancy measured and predicted between the proposed  $p$ - $y$  curve load-displacement relationships, the general shape of the curves is very similar, indicating that the small discrepancy may be due to overestimation of secant modulus  $E_{50}$ .

*Case 2.* The results calculated by the proposed method and the results calculated by Georgiadis and Georgiadis [17], which presented 3D finite-element analyses of pile in sloping ground, are presented in Figure 7 for comparison purposes. This paper selects two different slope angles ( $\theta = 20^\circ, 40^\circ$ , respectively) for verification analysis. As the slope angle increases, the results of this method are getting closer to the results of the literature [17].

*Case 3.* The calculating results given by Georgiadis and Georgiadis [18] are used as examples for comparison verification. Pile foundation is completely buried in the undrained clay slope. Thus, the section of the pile head at ground surface only has the initial horizontal force  $H_0$ . This paper selects four different pile's distance from slope crest ( $B = 0.3$  m, 0.6 m, 1.2 m, 2.4 m, respectively) for verification analysis. The  $H_0$ - $y_0$  curves and  $H_0$ - $\max M$  curves of pile head obtained from the proposed method and literature [18] are plotted in Figure 8. A good agreement has been observed between the calculating results from the present study and literature results.

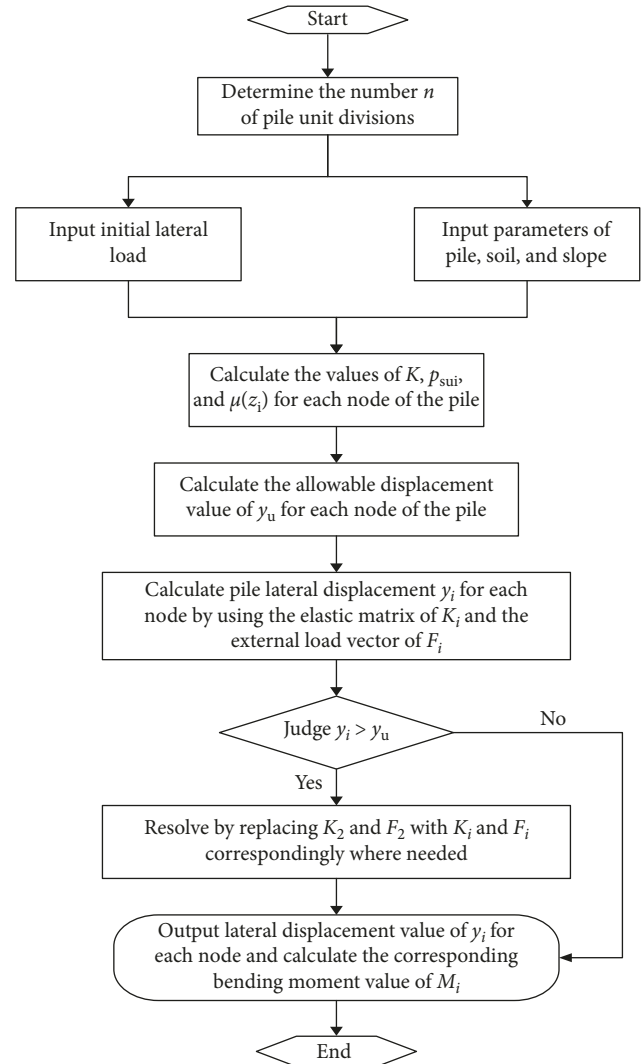


FIGURE 5: Flowchart of iterative calculation.

## 8. Parametric Study

*8.1. Effect of Slope Angle  $\theta$ .* The size of the slope angle directly determines the soil volume in front of the pile to participate in the pile-soil interaction. In order to better show the effect of slope angles, the pile head deflection of slope was normalized by dividing the pile head deflection of slope ( $y_{0,s}$ ) by that of horizontal ( $y_{0,H}$ ). Figures 9–12, respectively, show the lateral load-deflection curves at pile head, the normalized deflection ( $y_{0,s}/y_{0,H}$ )-load ( $H_0$ ) curves at pile head  $y_0$ , the maximum bending moment ( $M_{\max}$ )-load ( $H_0$ ) curves, and the bending moment ( $M$ )-depth ( $z$ ) distribution curves with different slope angles of  $0^\circ, 10^\circ, 20^\circ, 40^\circ, 50^\circ$ . The relevant calculation parameters here are pile length  $L = 14$  m, pile diameter  $D = 0.6$  m, bending stiffness of pile  $E_p I_p = 184.49$  (MN·m<sup>2</sup>), normalized distance of pile  $B/D = 0.5$ , adhesion coefficient  $\alpha = 1$ ; piles are completely buried in undrained clay, and Poisson's ratio of clay  $\nu_s = 0.49$ , undrained shear strength  $c_u = 40$  kPa, and secant modulus  $E_{50} = 14$  MPa.

As shown in Figure 9, as the slope angle increases, the lateral deflection of the pile head increases significantly, and

TABLE 1: Summary of pile load test.

Pile test	Geometrical characteristics							Soil properties			
	$L$ (m)	$D$ (m)	$B$ (m)	$E_p I_p$ (kN·m)	$e$ (m)	$\theta$ (deg)	$c_u$ (kPa)	$E_{50}$ (kPa)	$\gamma$ or $\gamma'$ (kN/m <sup>3</sup> )	$\alpha$	
1	14	0.5	0	97900	0.72	0	30	3000	7	0.94	
2	20	1.0	0	1423534	0	20,40	70	14000	18	0.5	
3	12	0.6	0.3, 0.6, 1.2, 2.4	184490	0	45	50	10000	18	0.73	

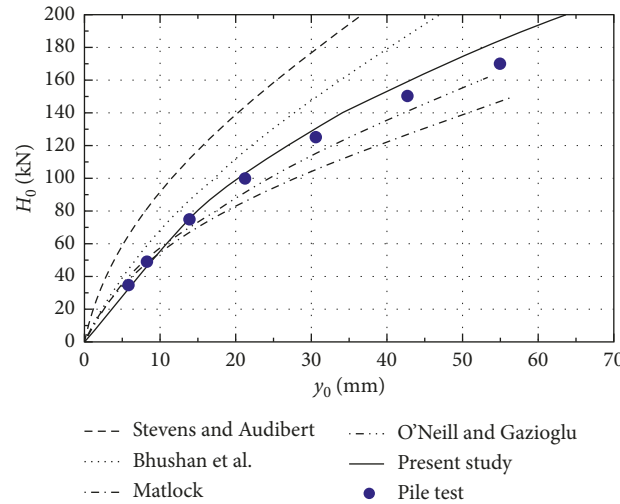


FIGURE 6: Verification analysis of  $H_0$ - $y_0$  curves relationship for Shanghai pile tests.

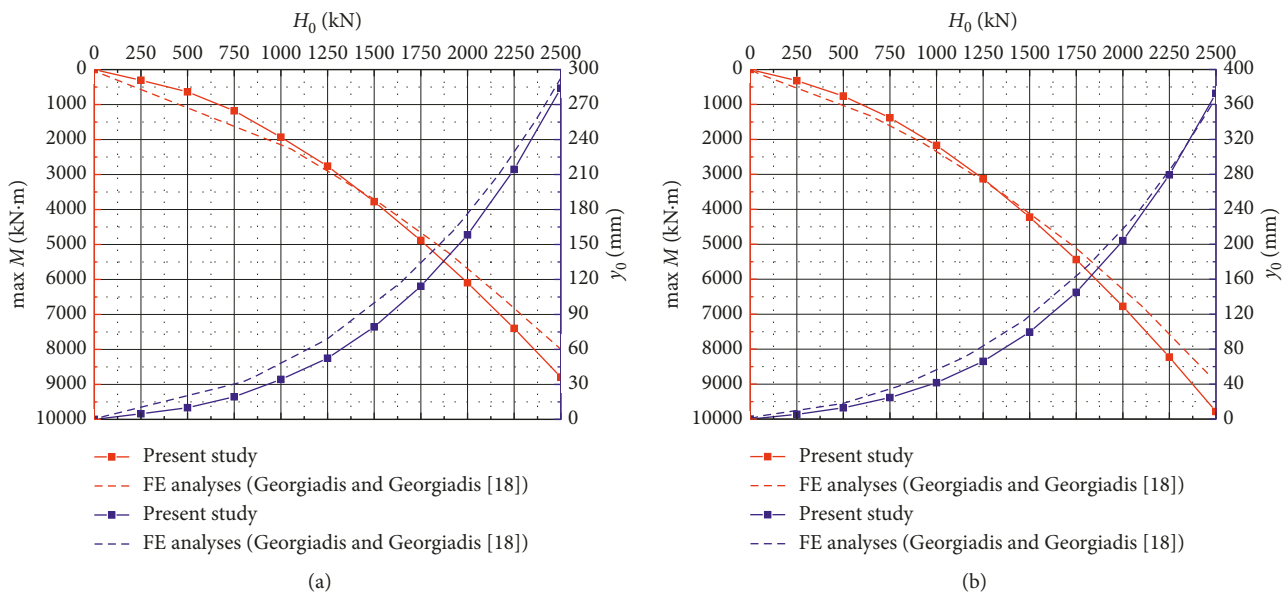


FIGURE 7: Verification analysis of  $H_0$ - $y_0$  curves relationship for FE analysis. (a)  $\theta = 20^\circ$  (b)  $\theta = 40^\circ$ .

this trend becomes much more obvious with the increase of the lateral load. It is also observed that when ground surface changes from horizontal ground to  $10^\circ$  slope, the behavior of pile is almost like horizontal ground surface, indicating the effect of slope is almost negligible when the slope angle is  $<10^\circ$ . Figure 10 further shows the distribution curves of normalized deflection ( $y_{0,s}/y_{0,H}$ ) with the lateral load. It can be seen that different fixed ratios of  $y_{0,s}/y_{0,H}$  are almost maintained at low load levels, but as the lateral load continue to increase, the

values of  $y_{0,s}/y_{0,H}$  start to increase unequally for different slope angle with the increase of load. When the lateral load is at 750 kN, the values of  $y_{0,s}/y_{0,H}$  for  $40^\circ$  slope and  $50^\circ$  slope are 1.065, 2.157, respectively, indicating that the steeper the slope angle is, the more deflection of pile head grows.

It can be seen from Figure 11 that the maximum bending moment values of the pile also increase as the slope angle increases, but the rate of increase of maximum bending moment with lateral load is more moderate.

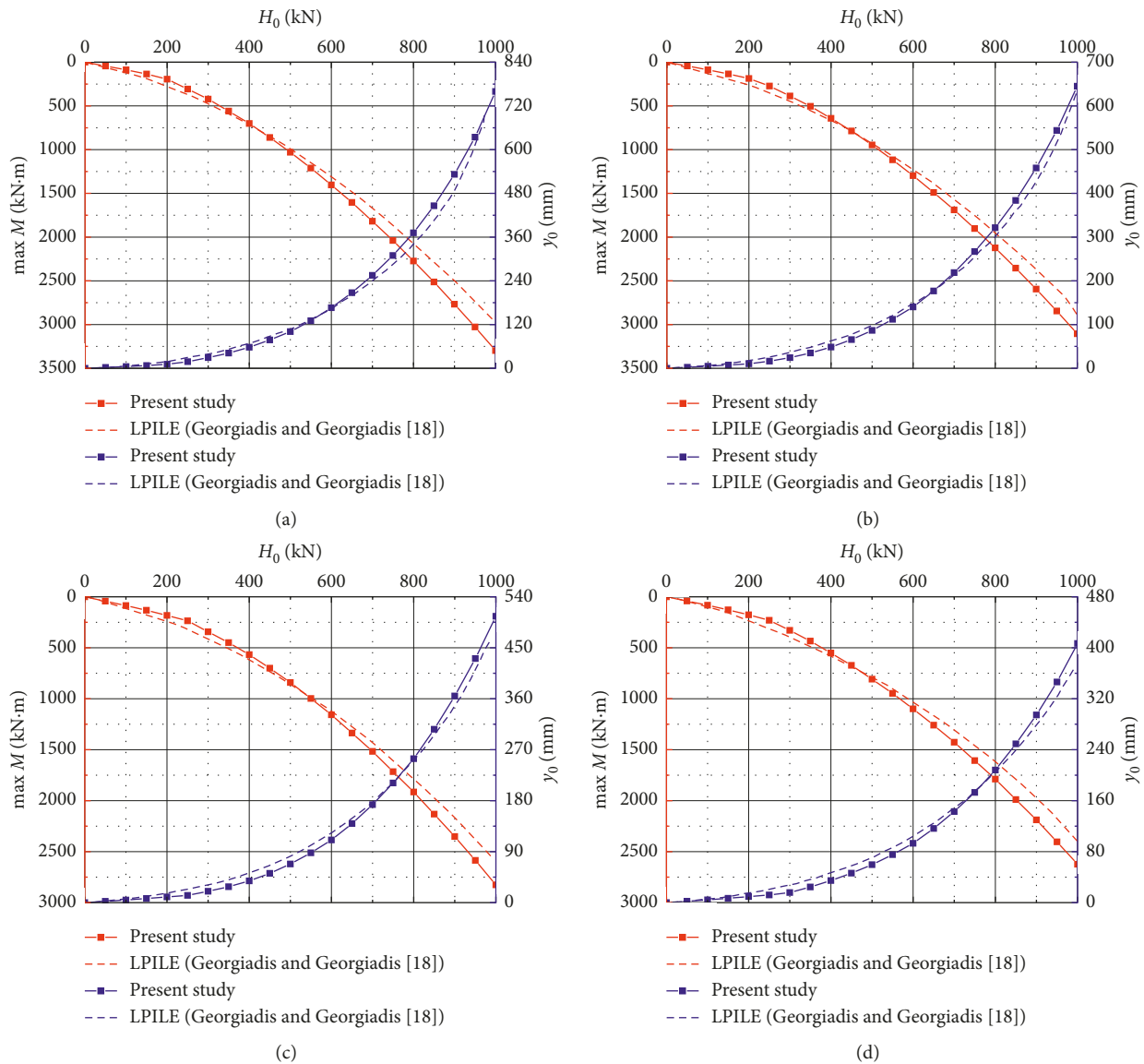


FIGURE 8: Verification analysis of  $H_0$ - $y_0$  curves relationship for LPILE. (a)  $B = 0.3$  m, (b)  $B = 0.6$  m, (c)  $B = 1.2$  m, (d)  $B = 2.4$  m.

Figures 12 and 13 show the bending moment distribution with depth and the depth of fixity (where the maximum bending moment occurs) of the pile for all slope angles with a lateral load at 300 kN and 600 kN, respectively. It is clear that the maximum bending moment of the pile increases with the increase of slope angle at the same load, but the first zero location of bending moment curve and depth of fixity increase correspondingly. With the increase of the load, the difference in the maximum bending moment growth at each slope angle becomes obvious, and the first zero location of bending moment curve and depth of fixity of the pile also increase more quickly. For example, as is shown in Figure 13, the depth of fixity for 30° and 50° slope angle increased by 4.46%, 17.34% compared with that in horizontal ground at the load of 300 kN, respectively, but the ratio further increases to 11.32%, 32.03%, respectively, when the load increases to 600 kN. It can also be seen from Figure 13 that the depth of pile fixity almost occurs at a depth of 4~8D ( $D =$  diameter of pile).

8.2. *Effect of Normalized Distance of Pile B/D.* Selecting the normalized distance of pile  $B/D$  as 0.5, 2, 4, 6, and consider the slope angle of 10°, 30°, 50°, respectively, as the existing slope conditions. The other calculation parameters are the same as in Section 8.1.

Figures 14–16 show the load-deflection curve for different normalized distance  $B/D$  of pile head at above three slope conditions. From these figures, it is observed that the increase in normalized distance  $B/D$  ratio decreases the deflection of pile head. When normalized distance  $B/D$  ratio exceeds 6 in all slope angle conditions, the deflection at pile head is basically the same as that in horizontal ground, which means the influence of the slope effect is almost negligible in this case. It is also observed that the load-deflection curves in different slope angle conditions have different response results, and the increase in slope angle can increase the discreteness of the curves. Figure 17 further shows the effect of normalized distance of pile on

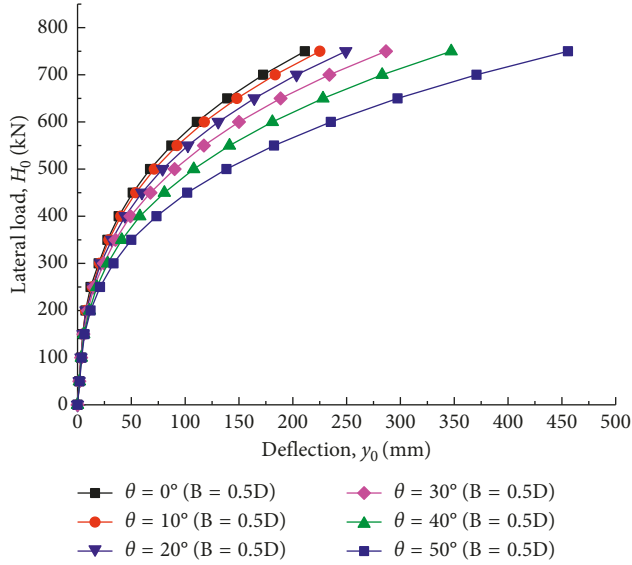


FIGURE 9: Lateral load-deflection curves for different slope angle at pile head.

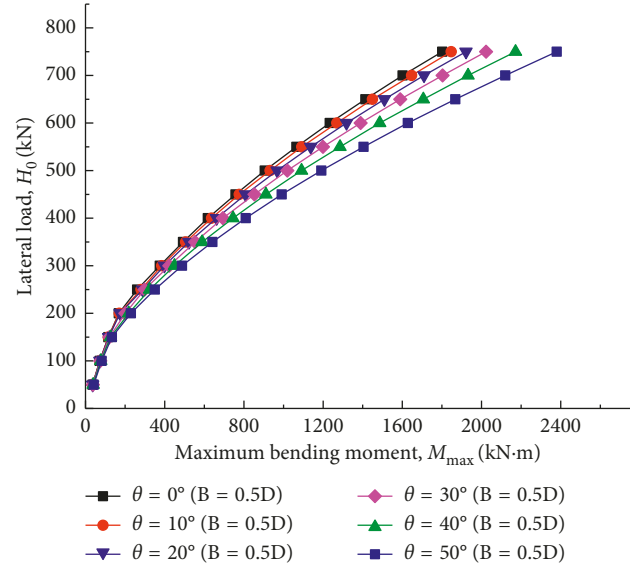


FIGURE 11: Maximum bending moment-load curves for different slope angle.

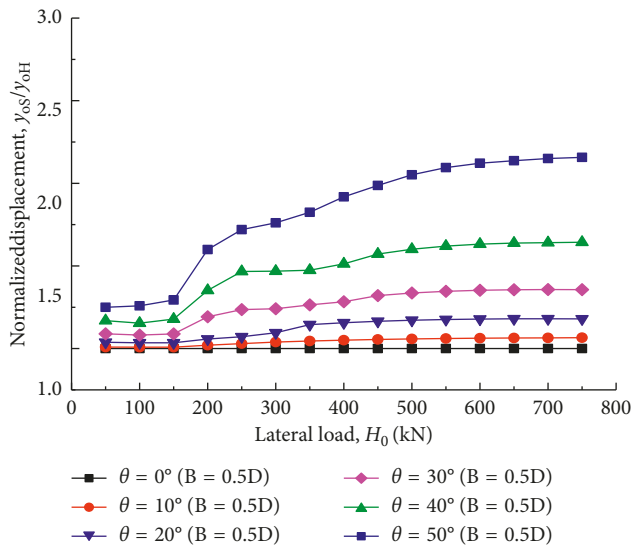


FIGURE 10: Normalized deflection ( $y_{0,s}/y_{0,H}$ )-load ( $H_0$ ) curves for different slope angle.

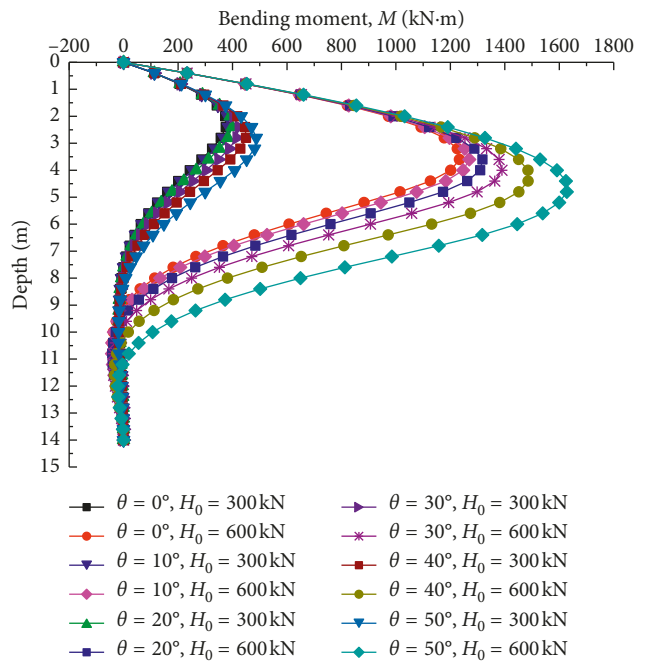


FIGURE 12: Bending moment variation along the depth of pile for different slope angle.

lateral-load capacity on horizontal ground and sloping ground ( $\theta = 10^\circ, 30^\circ, 50^\circ$ ). It can be seen that when the normalized distance  $B/D$  of pile changes from 0.5 to 6, the lateral-load capacity is increased by 2.27%, 11.1%, 29.87% on  $10^\circ, 30^\circ, 50^\circ$  sloping ground, respectively, indicating that the increase in slope angle increases the influence of  $B/D$  on the lateral-load capacity of the pile.

Figures 18–20 show the bending moment variation along pile length of the pile for different normalized distance  $B/D$  on horizontal ground and sloping ground ( $\theta = 10^\circ, 30^\circ, 50^\circ$ ). From these figures, it is observed that the maximum bending moment increases with the increase in the normalized distance  $B/D$  of the pile and the increase in the applied lateral load. Also, for the same normalized

distance  $B/D$  of pile and applied lateral load, the increase in slope angle of  $\theta$  increases the maximum bending moment of pile. When ground surface changes from horizontal to  $10^\circ, 30^\circ$ , and  $50^\circ$  sloping ground, the maximum bending moment of pile in sloping ground is increased by 2.8%, 12.6%, and 31.9%, respectively, under lateral load of 600 kN and normalized distance  $B/D$  of 0.5. It is also noted that when the pile is nearer to slope crest, the slope angle becomes a more dominant factor to affect the lateral capacity of the pile, especially at a high-load level.

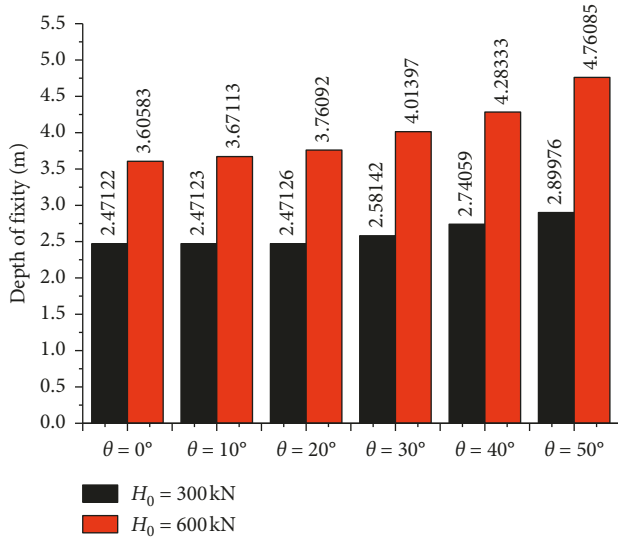


FIGURE 13: Depth of fixity variation with different slope angle.

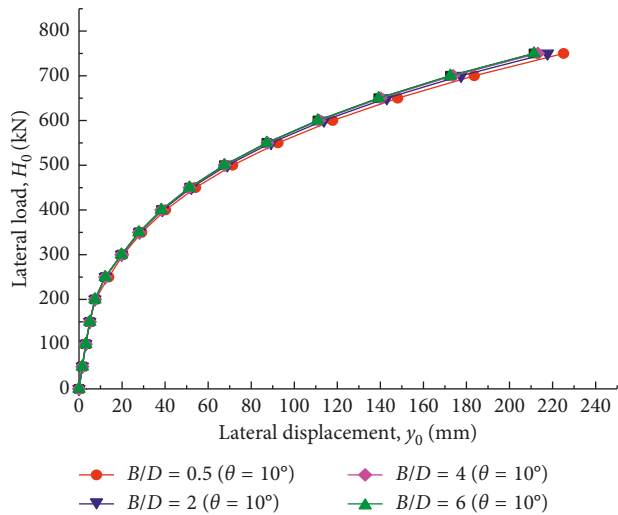


FIGURE 14: Lateral load-deflection curves for  $\theta = 10^\circ$  for different normalized distance of pile at pile head.

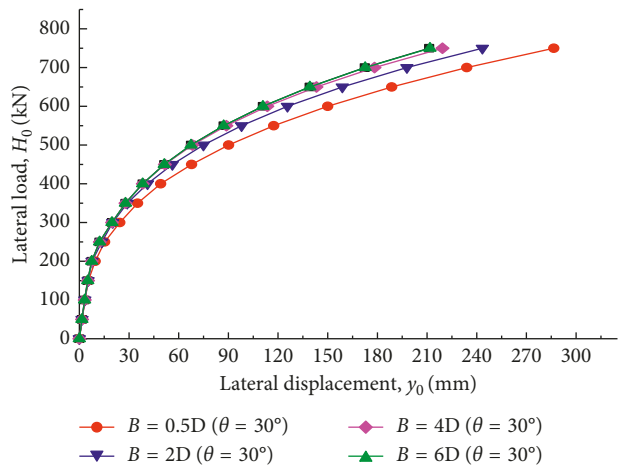


FIGURE 15: Lateral load-deflection curves for  $\theta = 30^\circ$  for different normalized distance of pile at pile head.

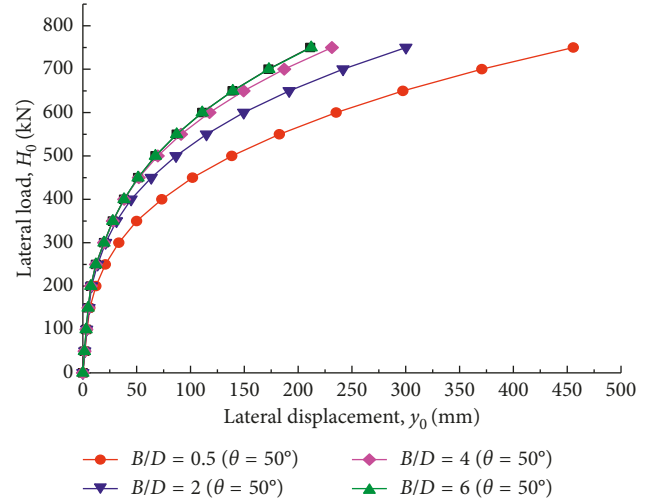


FIGURE 16: Lateral load-deflection curves for  $\theta = 50^\circ$  for different normalized distance of pile at pile head.

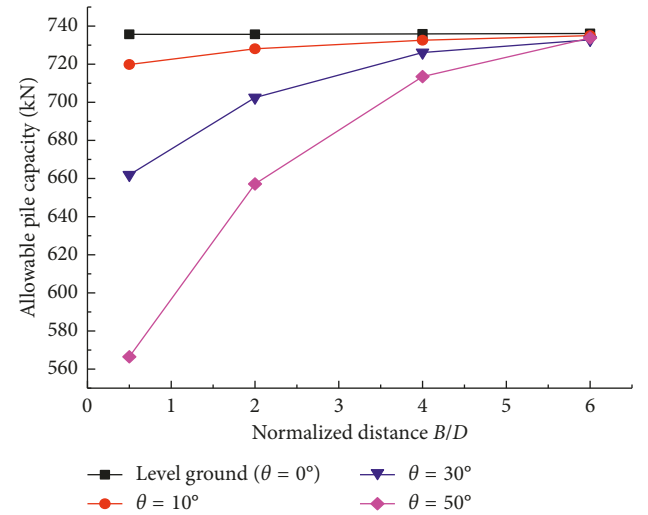


FIGURE 17: Bearing capacity of pile head for different normalized distance of pile (corresponding to 200 mm).

8.3. *Effect of Adhesion Coefficient  $\alpha$ .* In order to study the effect of adhesion coefficient  $\alpha$  on the lateral behavior of pile in sloped ground, this paper analyzes the parameter  $\alpha$  from 0 to 1, with increment of 0.1, and chooses lateral load  $H_0 = 500\text{ kN}$  and the bending moment  $M_0 = 0\text{ (kN}\cdot\text{m)}$  as the fixed loading condition to calculate and analyze the deflection of pile head. Consider the slope angle  $\theta$  as the same in Section 8.1, and other basic calculation parameters are the same as Section 8.1.

Figures 21 and 22 show pile head deflection ( $y_0$ ) and the maximum bending moment ( $M_{\max}$ ) of the pile variation with the adhesion coefficient  $\alpha$  for different slope angle, respectively. From these figures, it can be seen that increasing the adhesion coefficient  $\alpha$  at the pile-soil interface can effectively reduce the pile head deflection and the maximum bending moment of the pile at the same time. Also, the increase in slope angle almost does not change the corresponding curve growth model but will significantly increase

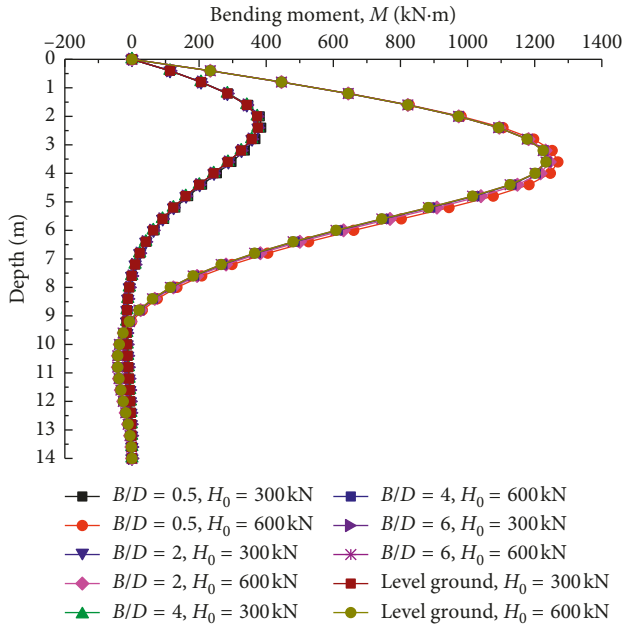


FIGURE 18: Bending moment variation along the depth of pile for  $\theta = 10^\circ$  for different slope angle.

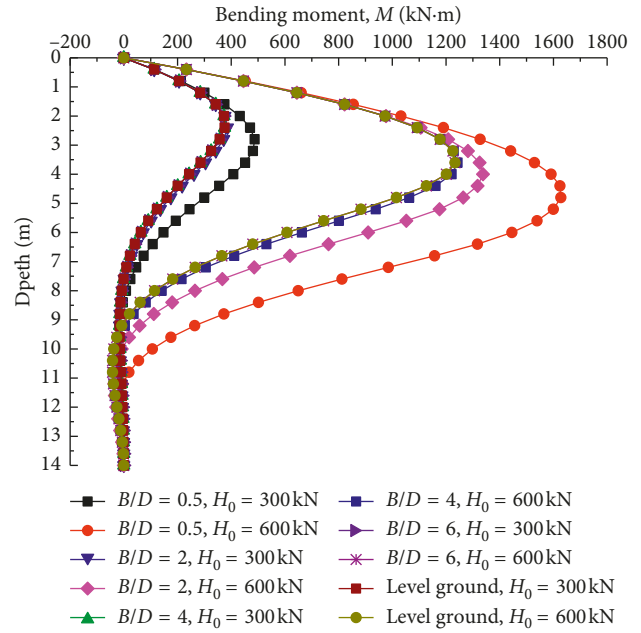


FIGURE 20: Bending moment variation along the depth of pile for  $\theta = 50^\circ$  for different slope angle.

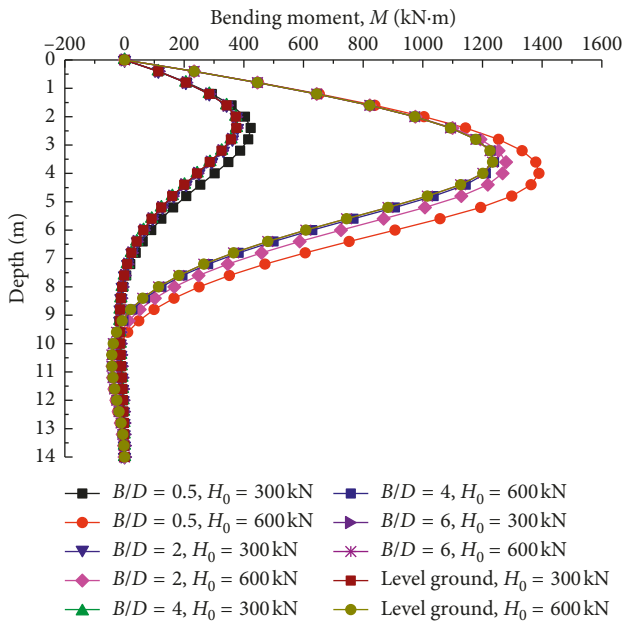


FIGURE 19: Bending moment variation along the depth of pile for  $\theta = 30^\circ$  for different slope angle.

the pile head deflection and maximum bending moment of the pile especially when the slope angle exceeds  $40^\circ$ . An example is used for pile head deflection, when the value of  $\alpha$  is equal to 0, the pile head deflection values of pile in sloping ground with  $\theta = 10^\circ, 30^\circ, 50^\circ$  is increased by 7.4%, 39.8%, 137%, respectively, compared to that in horizontal ground.

8.4. Effect of Undrained Shear Strength  $c_u$ . Here, lateral load  $H_0 = 500$  kN and the initial bending moment  $M_0 = 0$  (kN-m)

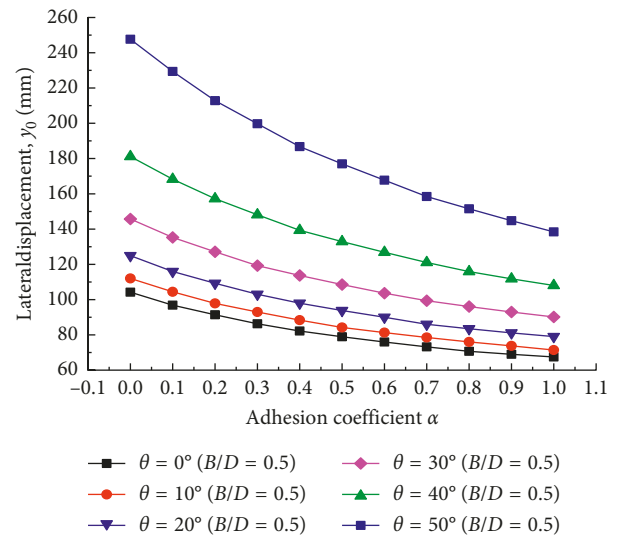


FIGURE 21: Pile head deflection ( $\gamma_0$ ) variation with adhesion coefficient ( $\alpha$ ) for different slope angle.

were taken as the initial loading conditions, choosing undrained shear strengths  $c_u$  of 20 kPa, 40 kPa, 60, 80 kPa, 100 kPa, respectively, to calculate and analyze. Other basic calculation parameters are the same as in Section 8.1.

Figures 23 and 24 show pile head deflection ( $\gamma_0$ ) and the maximum bending moment ( $M_{max}$ ) of the pile variation with the undrained shear strength  $c_u$  for different slope angles, respectively. From the curves given in Figures 23 and 24, it is observed that the increase in undrained shear strength  $c_u$  decreases the pile head deflection and the maximum bending moment. This is because of the increase in the strength of soil and the relative stiffness of the pile-soil system. Also, it is obvious that the presence of slopes

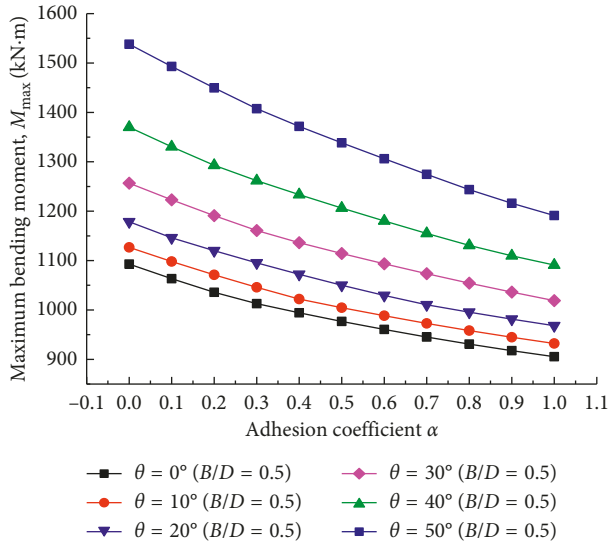


FIGURE 22: Maximum bending moment ( $M_{max}$ ) variation with adhesion coefficient ( $\alpha$ ) for different slope angle.

aggravates the rate of change of pile head deflection, especially when  $c_u$  ranges from 20 kPa to 40 kPa, and when the value of  $c_u$  exceeds 40 kPa, the decrease rate of the deflection of pile head becomes slow and eventually almost becomes flat. From the results in Figure 23, it is observed that the pile head deflection in the range of 73.4%–75% for increase in  $c_u$  20 kPa to 40 kPa of sloping ground ( $\theta = 10^\circ, 20^\circ, 30^\circ, 40^\circ, 50^\circ$ ) and horizontal ground surfaces, from which can conclude that the weaker soil parameters are, the more significant slope effect becomes. Besides, the curve of the maximum bending moment variation with undrained shear strength shown in Figure 24 is smoother, and the range of the maximum bending moment of the pile with the increase of the slope is relatively stable.

### 9. Conclusions

The purpose of this paper is to study the behavior of laterally loaded long-flexible pile in undrained clay sloping ground. Based on the basic model of ideal elastic-plastic  $p$ - $\gamma$  curve method, this paper derives the differential equations of the laterally loaded single pile in undrained clay sloped ground by introducing the existing related reduction variable function, and the corresponding finite difference method for the pile deflection and internal force is obtained. A series of parameters analyses are further performed for slope angle, normalized distance of pile, adhesion coefficient, and undrained shear strength. The conclusions obtained from this study are summarized as follows:

- (1) A nonlinear analysis method for laterally loaded long-flexible pile in undrained clay sloped ground is established. Through the verification of examples, the correctness and feasibility of the method is proved.
- (2) Slope angle is the most important factor that affecting the lateral bearing capacity of the near-slope pile. The increase in slope angle increases the deflection and the

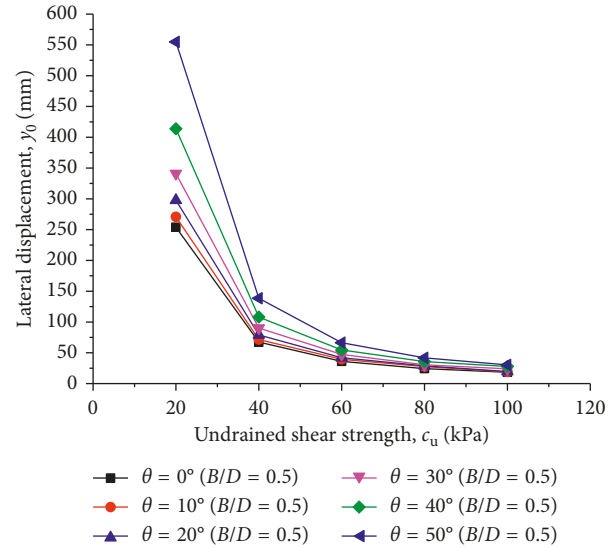


FIGURE 23: Pile head deflection ( $y_0$ ) variation with undrained shear strength ( $c_u$ ) for different slope angle.

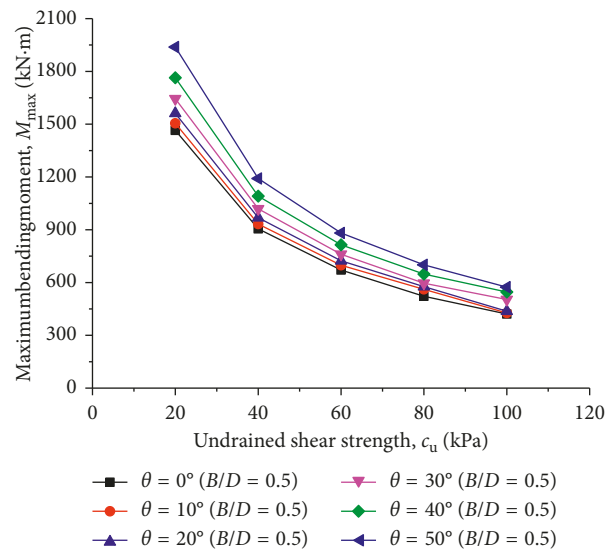


FIGURE 24: Maximum bending moment ( $M_{max}$ ) variation with undrained shear strength ( $c_u$ ) for different slope angle.

rate of increase of deflection, and this trend becomes more obvious as the lateral load increased. When the slope angle is small enough ( $\theta < 10^\circ$ ), the effect of slope is almost negligible. Besides, the depth of fixity of the pile is about 4–8 times the size of the pile diameter.

- (3) The distance away from pile to slope crest is also an important factor that affects the lateral-load capacity of the pile. The increase in normalized distance  $B/D$  of the pile decreases the deflection of pile head but increases the lateral-load capacity, and when normalized distance  $B/D$  ratio exceeds 6, the slope effect can be avoided. When laterally loaded pile is closer to the slope crest, the influence of the slope angle seems more dominant.

- (4) The adhesion coefficient  $\alpha$  at the pile-soil interface can effectively reduce the pile head deflection and the maximum bending moment of the pile at the same time. The increase in slope angle will significantly increase the pile head deflection and maximum bending moment of the pile especially when the slope angle exceeds  $40^\circ$ .
- (5) The increase in undrained shear strength  $c_u$  decreases the pile head deflection and the maximum bending moment of the pile. This is because of the increase in the strength of soil and the relative stiffness of the pile-soil system. Also, the presence of slopes aggravates the rate of change of pile head deflection, especially when the  $c_u$  is in a small value (ranges from 20 kPa to 40 kPa). In contrast, the maximum bending moment variation with undrained shear strength affected by the slope effect appears more moderate.
- (6) This study researches the lateral bearing behavior of single pile in undrained clay sloping ground. In practical projects, the situation of pile foundations on slope ground surface is not uncommon, and the lateral bearing characteristics of pile foundations are more complicated. Therefore, the influence of slope effect on the lateral bearing capacity of pile which is on slope ground surface is worth further study.

### Data Availability

The original data for summary of pile load test in Table 1 are from Wu et al. [28], Georgiadis and Georgiadis [17], and Georgiadis and Georgiadis [18], respectively. The computed pile responses, as shown in Figure 6, are compared to the pile test results (Wu et al. [28]) and to the pile responses computed with the same computer code using as input the Matlock [2]; Reese and Welch [5]; Bhushan et al. [26]; Stevens and Audibert [27]. Figures 7 and 8 are calculated by computer code MATLAB to compare previous studies (Georgiadis and Georgiadis [17], Georgiadis and Georgiadis [18], respectively). Figures 9–24 are calculated by the proposed method based on the original data mentioned above to study parametric analysis. In addition, all the sharing data were involved in this paper, and there was no redundant data.

### Conflicts of Interest

The authors declare that there are no conflicts of interest regarding the publication of this paper.

### Acknowledgments

This work is supported by the National Natural Science Foundation of China (grant nos. 51478479 and 51678570) and Hunan Transport Technology Project (grant no. 201524).

### References

- [1] N. Nimityongskul, Y. Kawamata, D. Rayamajhi, and S. A. Ashford, "Full-scale tests on effects of slope on lateral capacity of piles installed in cohesive soils," *Journal of Geotechnical and Geoenvironmental Engineering*, vol. 144, no. 1, article 04017103, 2018.
- [2] H. Matlock, "Correlation for design of laterally loaded piles in soft clay," in *Proceedings of the Offshore Technology Conference*, pp. 77–94, Houston, TX, USA, April 1970.
- [3] L. C. Reese, "Analysis of laterally loaded piles in sand," in *Proceedings of the Offshore Technical Conference*, pp. 95–105, Houston, TX, USA, May 1974.
- [4] L. Reese, W. Cox, and F. Koop, "Field testing and analysis of laterally loaded piles on stiff clay," in *Proceedings of the Offshore Technology in Civil Engineering*, pp. 106–125, Dallas, TX, USA, May 1975.
- [5] L. C. Reese and R. C. Welch, "Lateral loading of deep foundations in stiff clay," *Journal of Geotechnical and Geoenvironmental Engineering*, vol. 101, no. 7, pp. 633–649, 1975.
- [6] M. A. Gabr, T. Lunne, and J. J. Powell, "P-y analysis of laterally loaded piles in clay using DMT," *Journal of Geotechnical Engineering*, vol. 120, no. 5, pp. 816–837, 1994.
- [7] C. C. Fan and J. H. Long, "Assessment of existing methods for predicting soil response of laterally loaded piles in sand," *Computers and Geotechnics*, vol. 32, no. 4, pp. 274–289, 2005.
- [8] G. P. Yang and Z. M. Zhang, "Research on P-Y curve of laterally bearing piles under large displacement," *Water Transportation Engineering*, vol. 342, no. 7, pp. 40–45, 2002.
- [9] C. Wang and Z. A. LU, "Calculation of internal forces of laterally loaded piles by using p-y curve," *Journal of Chongqing Jiaotong University (Natural Science)*, vol. 4, no. 1, pp. 61–65, 1958.
- [10] H. C. Wang and D. Q. WU, "A new unified approach to the p-y curve of laterally loaded pile in clay," *Journal of Hohai University*, no. 1, pp. 9–17, 1991.
- [11] G. C. Wang and M. Yang, "Nonlinear analysis of laterally loaded piles in sand," *Rock and Soil Mechanics*, no. 2, pp. 261–267, 2011.
- [12] G. C. Wang and M. Yang, "Calculation of laterally loaded piles in clay," *Journal of Tongji University (Natural Science)*, vol. 40, no. 3, pp. 373–378, 2012.
- [13] T. Q. Zhou, Z. A. LU, and D. H. Wang, "Calculation method of laterally loaded super-long PHC pile," *Port and Waterway Engineering*, no. 6, pp. 155–160, 2013.
- [14] L. U. Cheng, X. C. Xu, S. X. Chen et al., "Model test and numerical simulation of horizontal bearing capacity and impact factors for foundation piles in slope," *Rock and Soil Mechanics*, no. 9, pp. 2685–2691, 2014.
- [15] P. YinB, H. ZhaoM, H. Zhao et al., "Stability analysis of pile-column bridge pile considering slope effect," *Journal of Hunan University (Natural Science)*, vol. 43, no. 11, pp. 20–25, 2016.
- [16] Y. S. Deng, M. H. Zhao, X. J. Zhou et al., "Research progress of bearing characteristics of pile column at steep slope in mountain areas," *Journal of Highway and Transportation Research and Development*, vol. 29, no. 6, pp. 37–45, 2012.
- [17] K. Georgiadis and M. Georgiadis, "Undrained lateral pile response in sloping ground," *Journal of Geotechnical and Geoenvironmental Engineering*, vol. 136, no. 11, pp. 1489–1500, 2010.
- [18] K. Georgiadis and M. Georgiadis, "Development of p-y, curves for undrained response of piles near slopes," *Computers and Geotechnics*, vol. 40, no. 3, pp. 53–61, 2012.

- [19] K. Muthukkumaran, R. Sundaravadivelu, and S. R. Gandhi, "Effect of slope on p-y curves due to surcharge load," *Soils and Foundations*, vol. 48, no. 3, pp. 353–361, 2008.
- [20] L. M. Zhang, C. W. W. Ng, and C. J. Lee, "Effects of slope and sleeving on the behavior of laterally loaded piles," *Soils and Foundations*, vol. 44, no. 4, pp. 99–108, 2008.
- [21] B. P. Yin, M. H. Zhao, W. He et al., "Model test study on identification of foundation proportional coefficient m in slope ground," *Journal of Hunan University (Natural Science)*, vol. 44, no. 9, 2017.
- [22] B. L. Gao, C. R. Zhang, and Z. X. Zhang, "Model tests on effect of slopes on lateral resistance of near single piles in sand," *Rock and Soil Mechanics*, vol. 35, no. 11, pp. 3191–3198, 2014.
- [23] B. T. Zhu, *The Ultimate Resistance and Laterally Loaded Pile Behaviors*, Tongji University School of Civil Engineering, Shanghai, China, 2005.
- [24] S. S. Rajashree and T. G. Sitharam, "Nonlinear finite-element modeling of batter piles under lateral load," *Journal of Geotechnical and Geoenvironmental Engineering*, vol. 127, no. 7, pp. 604–612, 2001.
- [25] R. L. Kondner, "Hyperbolic stress-strain response: cohesive soils," *Journal of the Soil Mechanics and Foundations Division*, vol. 89, no. 1, pp. 115–143, 1963.
- [26] K. Bhushan, S. C. Haley, and P. T. Fong, "Lateral load tests on drilled piers in stiff clays," *Journal of the Geotechnical Engineering Division*, vol. 1058, pp. 969–985, 1979.
- [27] J. B. Stevens and J. M. E. Audibert, "Re-examination of P-Y curve formulations," in *Proceedings of 11th Offshore Technology Conference*, pp. 397–403, Houston, TX, USA, 1980.
- [28] D. Wu, B. B. Broms, and V. Choa, "Design of laterally loaded piles in cohesive soils using p-y curves," *Soils and Foundations*, vol. 38, no. 2, pp. 17–26, 1998.



**Hindawi**

Submit your manuscripts at  
[www.hindawi.com](http://www.hindawi.com)

